

## Polymer Flow Birefringence and Internal Viscosity

Mónica A. Fontelos,<sup>†</sup> Fabio Ganazzoli, and Giuseppe Allegra\*

Dipartimento di Chimica, Politecnico di Milano, Piazza Leonardo da Vinci 32,  
I-20133 Milano, Italy. Received November 23, 1988;  
Revised Manuscript Received April 1, 1989

**ABSTRACT:** Flow birefringence and viscoelastic spectra of atactic polystyrene in dilute solution are interpreted according to a theoretical scheme where the rotational energy barriers display their dissipative effect by resisting the propagation of conformational changes along the chain (internal viscosity). For small to intermediate frequencies a satisfactory agreement with experiment is obtained by using physically realistic parameters. In particular, the characteristic time for skeletal bond rotation  $\tau_0$  is in essential agreement with values derived from NMR, ESR, and dielectric relaxation experiments. As the frequency approaches  $\tau_0^{-1}$ , increasing deviations are observed. According to Lodge and Schrag (*Macromolecules* 1984, 17, 352), it is suggested that solvent organization around the polymer chains may be at the origin of the observed discrepancy.

## Introduction

Oscillatory flow birefringence (OFB) and viscoelasticity (VE) experiments have provided a large amount of interesting information on the dynamics of polymer chains in solution.<sup>1</sup> The theoretical interpretation of the results is rather complex as several, difficult-to-separate physical factors act together. Among them we stress the hydrodynamic interaction, the good-solvent effect, and the conformational and the dynamic rigidity of the chain; the last two factors may be respectively traced to space correlation among skeletal bonds and to bond rotational hindrance, also definable as internal viscosity.<sup>2-4</sup> In particular, respectively denoting by  $S^*(\omega)$  and  $\eta^*(\omega)$  the complex flow birefringence and the complex viscosity, and by  $S_s$  and  $\eta_s$  the corresponding real quantities applying to the pure solvent, the moduli and especially the phase angles of  $S^*(\omega) - \phi S_s$  and of  $\eta^*(\omega) - \eta_s$  ( $\phi$  being the solvent volume fraction) change with the radian frequency  $\omega$  in quite different ways. (Henceforth, we shall consider sufficiently dilute solutions so that  $\phi \simeq 1$ .) Sending the reader to the following section for a full definition of  $S^*(\omega)$  and of  $\eta^*(\omega)$ , it suffices here to remark that while the former depends on the orientation of the chain bonds with respect to the applied shear deformation, the latter depends on the orientation of the intramolecular tension.<sup>5</sup> Only for the classical bead-and-spring chain are the two quantities bound to be strictly proportional to one another. Whenever the conformational rigidity and, especially, the internal viscosity become nonnegligible, the proportionality is lost, so that  $S^*(\omega) - S_s$  and  $\eta^*(\omega) - \eta_s$  may provide different types of information on the chain dynamics.

It is the purpose of this paper to show that experimental OFB and VE results from dilute solutions of atactic polystyrene in Aroclor 1248<sup>6,7</sup> may be satisfactorily interpreted with a self-contained theoretical model proposed by two of us,<sup>2,3</sup> provided the applied frequency is lower than the inverse of the characteristic time for bond rotational relaxation. We believe the physical significance of the present model is enhanced by considering that in our calculations we adopt (i) a chain length equal to the sample average; (ii) a parameter for hydrodynamic interaction close to the one previously chosen by us on best-fitting criteria<sup>3</sup> and in the same range as found by other authors;<sup>6,7</sup> and (iii) a characteristic time for bond rotation relaxation  $\tau_0$  that is consistent with NMR, ESR, and dielectric relaxation results.<sup>8</sup> Besides, we neglect the (moderate)

good-solvent expansion in view of its modest effect upon chain dynamics.<sup>9</sup>

It has been objected that the present type of theoretical interpretation appears to conflict with experimental anomalies found with some polymers at relatively high frequencies, notably negative values of  $S'(\omega \rightarrow \infty) - S_s$  and/or of  $\eta'(\omega \rightarrow \infty) - \eta_s$  (where the prime denotes the in-phase component), as well as difficulties in obtaining frequency/temperature spectral superposition.<sup>10</sup> These high-frequency anomalies were traced to specific polymer-solvent interactions and according to Lodge and Schrag<sup>1,6,11</sup> might be effectively compensated by considering plots of  $S^*(\omega) - S'(\omega \rightarrow \infty)$  and  $\eta^*(\omega) - \eta'(\omega \rightarrow \infty)$  instead of  $S^*(\omega) - S_s$  and  $\eta^*(\omega) - \eta_s$  versus  $\omega$ , respectively. With this procedure, OFB and VE experiments would essentially provide the same dynamical information. (This issue was also considered in a more recent paper by Morris et al.<sup>11</sup>)

Unlike this kind of approach, we thought it useful to investigate the dynamical spectra along the more conventional Rouse-Zimm interpretation complemented with our version of the conformational rigidity<sup>12-14</sup> and the internal viscosity.<sup>2,3,13</sup> We shall see that agreement between calculations and experiment is satisfactory at low to intermediate frequencies but tends to break down as  $\omega$  approaches  $\tau_0^{-1}$ , in particular for  $\omega \geq 10^4 \text{ s}^{-1}$  (after reduction at  $T = 25^\circ \text{C}$ ,  $\eta_s = 1 \text{ P}$ ). In the last section we shall concisely discuss these deviations on the basis of the Lodge-Schrag assumption of specific polymer-solvent interactions.<sup>10</sup>

## The Internal Viscosity

If we stretch abruptly the ends of a long chain from an end-to-end distance  $R$  to  $R' > R$ , supposing both  $R$  and  $R'$  to be much less than the full chain extension, the applied force will not be immediately transmitted as an average tension to all chains bonds.<sup>2-4</sup> In fact (i), as is intuitive of a soft object like the polymer coil, at first the tension will be largest at the ends and will propagate toward the center; (ii) the tension being uniquely associated with the distribution of rotational states, it cannot travel faster than permitted by the effective relaxation time  $\tau_0$  for skeletal bond rotations, the limiting velocity being  $\propto \tau_0^{-1}$  bonds; and (iii) since the skeletal rotations are hindered by energy barriers, a dissipative, viscosity-like effect is to be expected. The problem was subjected to a nonequilibrium statistical-mechanical investigation, confirming the above conclusions.<sup>2,4</sup> The force arising within the chain from bond rotational relaxation is denoted as the *internal viscosity* (iv) force and the symbol  $\Phi(h,t)$  applies specifically to the iv force acting on the  $h$ th chain atom at time  $t$ . In the

<sup>†</sup>Permanent address: Comisión Nacional de Energía Atómica, Departamento de Reactores, Av. del Libertador 8250, 1429 Buenos Aires, Argentina.

linear approximation, its projection along  $x$  is given by<sup>4</sup>

$$\dot{\Phi}_x(h,t) + \Phi_x(h,t)/\tau_0 = \pm \frac{V}{2} \frac{d}{dt} \left[ \frac{\partial E}{\partial l_x(h,t)} + \frac{\partial E}{\partial l_x(h-1,t)} \right] \quad (1)$$

where  $E$  is the quadratic chain configurational potential and  $l_x(h,t)$  is the average projection along  $x$  of the bond adjoining the chain atoms labeled  $(h+1)$  and  $(h)$ . The pure number  $V$  is close to unity, its best estimate<sup>4</sup> being  $2/3$ . The sign ambiguity in the right-hand side is associated with the direction of energy (or tension) propagation along the chain. The present description requires that modes of chain motion consisting of standing waves be decomposed into a sum of oppositely traveling waves (see eq 12 and 13 in the following, e.g.). It is possible to show that the largest traveling velocity of any wave along the chain is  $(V\tau_0)^{-1}$  chain bonds/s, consistent with the requirement that the largest velocity of any rotational rearrangement must be  $\propto \tau_0^{-1}$ . Finally, the differential character of eq 1 implies that  $\Phi_x(h,t)$  be given by a memory integral in the full Langevin equation of motion, as may be seen in eq 16.

### Mathematical Formulation

The alternating shearing motion of the fluid is assumed to take place along the  $x$ -axis whereas the velocity gradient is along  $z$ . The chain is considered as either having an (...-A-A-A-...) structure or being effectively reduced to it.<sup>9</sup> There are  $N$  chain atoms, equivalent to  $(N-1)$  chain bonds. In agreement with the notation of Zimm,<sup>5</sup> denoting with  $r(h,t)$  ( $r = x, y, z$ ;  $h = 1, 2, \dots, N$ ) the general coordinate of the  $h$ th chain atom at time  $t$  and defining

$$\mathbf{x} = \begin{bmatrix} x(1,t) \\ x(2,t) \\ \vdots \\ x(N-1,t) \\ x(N,t) \end{bmatrix} \quad \mathbf{z} = \begin{bmatrix} z(1,t) \\ z(2,t) \\ \vdots \\ z(N-1,t) \\ z(N,t) \end{bmatrix}$$

$$\mathbf{A} = \begin{bmatrix} 1 & -1 & 0 & 0 & \dots & 0 & 0 & 0 \\ -1 & 2 & -1 & 0 & \dots & 0 & 0 & 0 \\ \vdots & \vdots & \vdots & \vdots & \dots & \vdots & \vdots & \vdots \\ 0 & 0 & 0 & 0 & \dots & -1 & 2 & -1 \\ 0 & 0 & 0 & 0 & \dots & 0 & -1 & 1 \end{bmatrix} \quad (2)$$

the magnitude of the birefringence of the solution is given by

$$\Delta n = \frac{Q\rho N_A}{NM_0} [(\langle \mathbf{x}^T \mathbf{A} \mathbf{x} \rangle - \langle \mathbf{z}^T \mathbf{A} \mathbf{z} \rangle)^2 + 4\langle \mathbf{x}^T \mathbf{A} \mathbf{z} \rangle^2]^{1/2} + \Delta n_s \quad (3)$$

where  $\Delta n_s$  is the solvent contribution;  $Q = (\gamma_1 - \gamma_2)/(3l^2)$  is an optical constant for the polymer;  $l$  is the bond length,  $\gamma_1$  and  $\gamma_2$  are the polarizability components per chain bond along the bond axis and at right angles, respectively;  $\rho$  is the polymer concentration in g/cm<sup>3</sup>;  $N_A$  is Avogadro's number; and  $M_0$  is the molar mass per chain atom. The alternating solvent velocity at point  $(x,y,z)$  is given by

$$v_x = z\gamma \exp(i\omega t), \quad v_y = v_z = 0 \quad (4)$$

Since we have, to within a good approximation in all practical cases

$$\langle \mathbf{x}^T \mathbf{A} \mathbf{x} \rangle \simeq \langle \mathbf{z}^T \mathbf{A} \mathbf{z} \rangle \quad (5)$$

due to the small deformation amplitude, we get from eq 3

$$S^*(\omega) = \frac{\Delta n}{\gamma \exp(i\omega t)} = \frac{2Q_1\rho}{N} \frac{\langle \mathbf{x}^T \mathbf{A} \mathbf{z} \rangle}{\gamma \exp(i\omega t)} + S_s \quad (6)$$

where

$$Q_1 = QN_A/M_0 \quad (6')$$

Concerning the complex viscosity, its general definition is

$$\eta^*(\omega) = \frac{\rho N_A}{NM_0} \frac{\langle \mathbf{f}_x^T \mathbf{T} \mathbf{z} \rangle}{\gamma \exp(i\omega t)} + \eta_s \quad (7)$$

where  $\mathbf{f}_x$  is the column vector containing the  $x$  components of the force exerted by the solvent upon the chain atoms and  $\eta_s$  is the solvent viscosity.

We must now evaluate the time evolution of  $x(h,t)$ ,  $z(h,t)$ , and  $f_x(h,t)$ . For this purpose, it is convenient at first to write down the Fourier transform producing the statistical normal modes for an open chain.<sup>5,13</sup> Projecting along  $x$ , e.g., we have

$$\tilde{x}(q,t) = 2^{1/2} \sum_{h=1}^N x(h,t) \cos [q(h - 1/2)]$$

$$q = n_q\pi/N, \quad n_q = 1, 2, \dots, N-1$$

$$\tilde{x}(0,t) = \sum_{h=1}^N x(h,t) \quad (8)$$

$$x(h,t) = 2^{1/2}/N \sum_{|q \neq 0|} \tilde{x}(q,t) \cos [q(h - 1/2)] + \tilde{x}(0,t)/N \quad (9)$$

$$\langle \tilde{x}(q,t) \tilde{x}(q',t) \rangle = [Nl^2/\mu(q)] \Delta(q - q') \quad (10)$$

$$\mu(q) = 4 \sin^2(q/2)/C(q) \quad (11)$$

where  $\Delta$  stands for the Kronecker delta. In the above, the chain configuration is decomposed in standing waves and  $C(q)$  is the generalized characteristic ratio.<sup>12,14</sup> This representation is not suited for direct introduction of the internal viscosity, and therefore we shall write<sup>13</sup>

$$x(h,t) = [x_+(h,t) + x_-(h,t)]/2^{1/2} \quad (12)$$

where  $x_+(h,t)$  and  $x_-(h,t)$  represent statistically independent chain motions propagating toward increasing and decreasing  $h$  values, respectively, with the same mean-square amplitude as  $x(h,t)$ . In turn, these may be Fourier-transformed as

$$x_{\pm}(h,t) = \frac{1}{2^{1/2}N} \sum_{|q \neq 0|} \{ \tilde{x}_{\pm}(q,t) \exp[iq(h - 1/2)] + \tilde{x}_{\pm}(-q,t) \exp[-iq(h - 1/2)] \} + \tilde{x}_{\pm}(0,t)/N \quad (13)$$

with the orthogonality relationships

$$\langle \tilde{x}_{\pm}(q,t) \tilde{x}_{\pm}(q',t) \rangle = [Nl^2/\mu(q)] \Delta(q + q') \quad (14)$$

$$\langle \tilde{x}_{\pm}(q,t) \tilde{x}_{\mp}(q',t) \rangle = 0 \quad (15)$$

where the last equation implies that different sets of Brownian forces contribute to  $\tilde{x}_+(q,t)$  and to  $\tilde{x}_-(q,t)$  separately. From eq 12 and 13, the stationary form of  $x(h,t)$  proposed in eq 9 is recovered. The Langevin equation producing  $\tilde{x}_{\pm}(q,t)$  is<sup>3,4</sup>

$$\frac{3k_B T}{l^2} \mu(q) \tilde{x}_{\pm}(q,t) \pm i \frac{3k_B T V \sin(q)}{C(q)l^2} \int_{-\infty}^t \tilde{x}_{\pm}(q,t') e^{-(t-t')/\tau_0} \times dt' + \zeta(q) [\tilde{x}_{\pm}(q,t) - \gamma e^{i\omega t} \tilde{z}_{\pm}(q,t)] = \tilde{X}_{\pm}(q,t) \quad (16)$$

where  $\tilde{X}(q,t)$  is the stochastic Brownian force,  $\tau_0$  is the characteristic time for skeletal bond rotation, and  $V$  is a constant number of order unity (see also eq 1;  $\Phi_x$  corresponds to the term with the memory integral) and<sup>15</sup>

$$\zeta(q) = \zeta/\nu(q) \quad (17)$$

$$\nu(q) = 1 + \frac{\zeta}{3\pi\eta_s N} \left(\frac{6}{\pi}\right)^{1/2} \sum_{h \neq j=1}^N \cos[q(h - \frac{1}{2})] \cos[q(j - \frac{1}{2})] \langle r^2(h, j) \rangle^{-1/2} \quad (18)$$

$$\langle r^2(h, j) \rangle = \frac{2l^2}{N} \sum_{|q \neq 0|} \frac{C(q) \sin^2[q(h - j)/2] \sin^2[q(h + j - 1)/2]}{\sin^2(q/2)} \quad (19)$$

$$\langle \tilde{X}_{\pm}(q, t) \tilde{X}_{\pm}(q', t') \rangle = Nk_B T \left\{ 2\zeta(q) \delta(t - t') \pm \frac{3k_B TV \sin(q) e^{-(t-t')/\tau_0}}{C(q)l^2} \right\} \Delta(q + q') \quad (20)$$

$$\langle \tilde{X}_{\pm}(q, t) \tilde{X}_{\mp}(q', t') \rangle = 0$$

In the above,  $r(h, j)$  stands for the distance between atoms  $h$  and  $j$ , and  $\zeta$  is the atomic friction coefficient. It should be reminded that the good-solvent expansion is neglected, so that all the normal modes have an expansion ratio equal to unity. Carrying out the calculations according to a previously discussed procedure,<sup>3</sup> we get from eq 6 and 7

$$S^*(\omega) = S_s + \frac{Q_1 \rho l^2}{3N} \sum_{|q'|} \frac{2\pi C(q')}{\tau_0(\omega_1 - \omega_2) \left[ \zeta(q') + \frac{3k_B T}{l^2} \mu(q') \tau_0 \right]} \times \left[ \frac{N_1(q', \omega_1 - \omega) P(q', \omega_1)}{M(q', \omega_1 - \omega) \omega_1} - \frac{N_1(q', \omega_2 - \omega) P(q', \omega_2)}{M(q', \omega_2 - \omega) \omega_2} \right] \quad (21)$$

$$\eta^*(\omega) = \eta_s + \frac{\rho N_A k_B T}{NM_0} \sum_{|q'|} \frac{\pi}{\tau_0(\omega_1 - \omega_2) \left[ \zeta(q') + \frac{3k_B T}{l^2} \mu(q') \tau_0 \right]} \times \left[ \frac{N(q', \omega_1 - \omega) P(q', \omega_1)}{M(q', \omega_1 - \omega) \omega_1} - \frac{N(q', \omega_2 - \omega) P(q', \omega_2)}{M(q', \omega_2 - \omega) \omega_2} \right] \quad (22)$$

where

$$q' = \pm n_q \pi / N, \quad n_q = 1, 2, \dots, N - 1 \quad (23)$$

$$\omega_1, \omega_2 = \frac{A(q) \mp [A^2(q) + B(q)]^{1/2}}{2\zeta(q)\tau_0} \quad (24a)$$

$$A(q) = \frac{3k_B T}{C(q)l^2} V \tau_0 \sin(q) + i \left[ \zeta(q) + \frac{3k_B T}{l^2} \mu(q) \tau_0 \right] \quad (24b)$$

$$B(q) = \frac{12k_B T}{l^2} \mu(q) \zeta(q) \tau_0 \quad (24c)$$

$$N_1(q, \omega) = \frac{3k_B T}{l^2} \mu(q) (1 - i\omega\tau_0) \quad (25a)$$

$$N(q, \omega) = N_1(q, \omega) + \frac{3k_B T}{C(q)l^2} V \omega \tau_0 \sin(q) \quad (25b)$$

$$M(q, \omega) = N(q, \omega) - i\omega\zeta(q)(1 - i\omega\tau_0) \quad (26)$$

$$P(q, \omega) = \frac{1}{2\pi} \left[ \zeta(q)(1 + \omega^2\tau_0^2) - \frac{3k_B T}{C(q)l^2} V \omega \tau_0^2 \sin(q) \right] \quad (27)$$

In the particular case  $\omega\tau_0 \ll 1$  the above expressions reduce to

$$S^*(\omega) = S_s + \frac{2Q_1 \rho l^2}{3N} \sum_{|q|} C(q) \frac{\tau(q)/2}{1 + i\omega\tau(q)/2} \quad (28)$$

$$\eta^*(\omega) = \eta_s + \frac{\rho N_A k_B T}{NM_0} \sum_{|q|} \left\{ 1 + \frac{i\omega 3k_B TV \tau_0^2 [1 + \cos(q)]}{2C(q)\zeta(q)l^2} \right\} \frac{\tau(q)/2}{1 + i\omega\tau(q)/2} \quad (29)$$

$$\tau(q) = \zeta(q)l^2 / 3k_B T \mu(q) \quad (30a)$$

$$\bar{\tau}(q) = \tau(q) \left\{ 1 + \left[ \frac{3k_B TV \tau_0 \sin(q)}{C(q)\zeta(q)l^2} \right]^2 \right\} \quad (30b)$$

where the set  $\{q\}$  of angles is again limited to the interval  $0-\pi$ ; see eq 8. Note that in the above expressions  $\tau(q)$  is the  $q$ -mode relaxation time in the absence of internal viscosity<sup>3,15</sup> and that we recover the classical bead-and-spring results for  $\tau_0/t_0 \rightarrow 0$ , where

$$t_0 = \zeta l^2 / k_B T \quad (31)$$

### Numerical Procedure

The numerical calculations were performed by using both the general expressions (21)–(27) and the simplified results (28)–(30) (for  $\omega\tau_0 \ll 1$ ). The generalized characteristic ratio for atactic polystyrene was taken from ref 9:

$$C(q) = \frac{0.0899}{1 - 0.990 \cos(q)} + 0.365 \quad (32)$$

Although quite accurate up to  $q \lesssim 0.5$  rad, this expression was used for simplicity in the whole  $q$  range since the relevant modes belong to small  $q$ .

Hydrodynamic interaction, embodied in  $\zeta(q)$ , was evaluated from eq 17–19. Since, however,  $\nu(q)$  changes rather slowly with  $q$ , we set in eq 19  $C(q) \approx \text{const} = C(0)$ , so that

$$\langle r^2(h, j) \rangle = C(0)l^2 |h - j| \quad (33)$$

Upon inserting this expression in the equation giving  $\nu(q)$  and replacing the double sum with integrals from 0 to  $N$ , we obtain<sup>15</sup>

$$\nu(q) = 1 + h_0 \left( \frac{8N}{n_q} \right)^{1/2} \left[ C(\pi n_q) - \frac{S(\pi n_q)}{2\pi n_q} \right] \quad (34a)$$

where

$$h_0 = \zeta / [6C(0)]^{1/2} \pi^{3/2} \eta_s l^2 \quad (34b)$$

and  $C(x)$  and  $S(x)$  are the Fresnel integrals defined by

$$C(x) = \frac{1}{(2\pi)^{1/2}} \int_0^x \frac{\cos(z)}{z^{1/2}} dz \quad (34c)$$

$$S(x) = \frac{1}{(2\pi)^{1/2}} \int_0^x \frac{\sin(z)}{z^{1/2}} dz$$

The numerical value of the parameters  $\tau_0$ ,  $t_0$ , and  $h_0$  was obtained by a fit with experimental results<sup>6,7</sup> from dilute solutions of atactic polystyrene in Aroclor 1248 reduced to 25 °C, where the solvent viscosity is  $\eta_s = 2.5$  P. We chose to obtain the best overall fit with the OFB results since these are the most accurate ones.<sup>1,6</sup> The number of chain atoms  $N$  was equal to the actual value, and  $l$  was taken as the C–C bond length, 1.54 Å. Concerning  $h_0$  (see eq 34b), it was treated as an adjustable parameter, ac-

cording to a common procedure,<sup>3</sup> in view of the uncertainties in the application of Stokes' law and of the preaveraging approximation for the Oseen tensor. The best-fitting value of  $h_0$  was found to be 0.055.

To the extent that Kramer's kinetic theory in the diffusive limit<sup>16</sup> applies to the chain rotational rearrangements and within the limited temperature range usually required by OFB and VE experiments, we have  $\tau_0 \propto \eta_s$ , whence, assuming  $\zeta \propto \eta_s$ ,  $\tau_0 \propto t_0$  in view of eq 31. The ratio  $V\tau_0/t_0$  was still given the previous value of 62.3, whereas, according to a recent analysis,<sup>4</sup> the numerical factor  $V$  was taken as  $2/3$  instead of  $4/3$  as in previous work.<sup>3</sup> From what precedes,  $t_0$  is the only time parameter and both  $S^*$  and  $\eta^*$  depend on the single variable  $\omega t_0$ .

By shifting the calculated curve of  $\varphi_s$ , that is the phase angle of  $S^*$  (see eq 35b), along the frequency axis to fit the experimental points, we could determine the value of the time unit  $t_0 = 2.06 \times 10^{-9}$  s, whence the friction coefficient per chain atom is  $\zeta = 3.57 \times 10^{-7}$  g s<sup>-1</sup>. From  $\zeta = 6\pi R_{\text{eff}}\eta_s$ , the effective radius  $R_{\text{eff}}$  of the chain atoms is 0.76 Å and from  $V\tau_0/t_0 = 62.3$ ,  $V = 2/3$ , the rotational relaxation time turns out to be  $\tau_0 = 1.92 \times 10^{-7}$  s. Calculation of the VE function was carried out with no further adjustment of parameters; only the number of chain atoms  $N$  was made to correspond to the average molecular weight  $M_w$  of the experimental sample.

## Results and Discussion

OFB and VE experiments are performed by applying a sinusoidally varying shear deformation to a sample solution. One can plot either the in-phase and the out-of-phase components as a function of the applied frequency or the modulus and the phase angle using a suitable phasor notation

$$\eta^* = \eta' - i\eta'' = \eta_M \exp(-i\varphi_\eta) + \eta_s \quad (35a)$$

$$S^* = S' - iS'' = S_M \exp(-i\varphi_s) + S_s \quad (35b)$$

We assume that  $\eta'$ ,  $\eta''$ ,  $\eta_M$ ,  $S'$ ,  $S''$ , and  $S_M$  are positive quantities; besides, the orientation of the laboratory frame and the difference  $\gamma_1 - \gamma_2$  between principal polarizabilities (giving the sign of  $Q_1$  in eq 21) are such that  $\varphi_\eta = \varphi_s = 0$  for  $\omega = 0$ , whereas  $\varphi_\eta$  and  $\varphi_s$  are positive for small  $\omega$ 's. (In the above, the primed and the double-primed terms give the dissipative and the elastic response, respectively.) OFB measurements are usually shown in the phasor notation,<sup>6</sup> whereas VE data are more often reported in the other notation, or in terms of the complex modulus,<sup>7</sup> defined as

$$G^* \equiv i\omega\eta^* = G' + iG'' \quad (35c)$$

The advantage of the phasor notation is that the phase angle is very sensitive to changes of chain structure or experimental conditions, such as concentration effects. On the other hand, only OFB experiments were reported to be sufficiently accurate to yield reliable values of  $\varphi$  even at high frequency.<sup>1,6</sup>

The difference between the two experiments is best seen when comparing  $\varphi_s$  and  $\varphi_\eta$ . In Figure 1 we report the calculated phase angles as a function of the applied frequency  $f = \omega/2\pi$  for a realistic set of parameters, i.e., those fitting the experimental results (see later). At small frequencies the two angles are equal: in this region  $S^*$  is proportional to  $\eta^*$ , only the most collective modes come into play and an equivalent bead-and-spring model with no internal viscosity may be employed. At larger frequencies,  $\varphi_s$  goes through a maximum, unlike  $\varphi_\eta$ , which reaches a minimum, and the simple proportionality between  $S^*$  and  $\eta^*$  is lost. As a consequence, the orientation of intramolecular stresses is no more identical with that

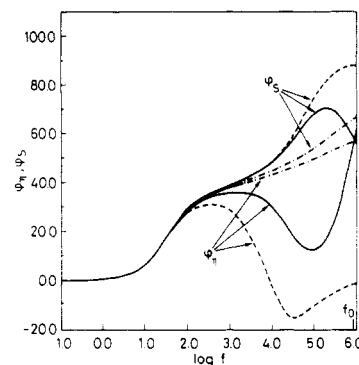


**Figure 1.** Phase angles  $\varphi_s$  and  $\varphi_\eta$  (see eq 35) as a function of the applied frequency in the presence of internal viscosity (from eq 21–27, solid lines); the results obtained with the simplified expressions (eq 28–30, dashed lines) and with no internal viscosity (i.e., with  $\tau_0 = 0$ , dash-and-dot lines) are also shown. Numerical values of the parameters are given in the text and the number of skeletal atoms  $N$  is  $7.5 \times 10^3$ , corresponding to  $M_w = 3.9 \times 10^5$  for polystyrene. The value of  $f_0 = (2\pi\tau_0)^{-1}$  is also shown.

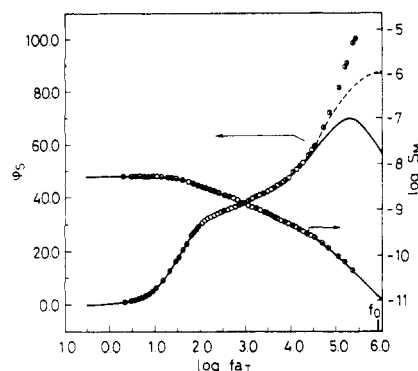


**Figure 2.** Experimental and calculated plot of  $\varphi_s$  and  $\log S_M$  (see eq 35) as a function of the applied frequency (solid lines). The shift factor  $a_T$  effectively reduces the experimental points to 25 °C; in our calculations we take  $T = 25$  °C and  $a_T = 1$ . The curve of  $\varphi_s$  calculated with the simplified expressions (eq 28–30) is also shown (dashed line). Experimental results are from atactic polystyrene,  $M_w = 3.9 \times 10^5$ , in Aroclor 1248 ( $\eta_s = 2.5$  P at  $T = 25$  °C),  $\rho = 0.0109$  g cm<sup>-3</sup> (from ref 6). Numerical values of the parameters are given in the text and  $N$  is  $7.5 \times 10^3$ . The characteristic frequency of skeletal rotation  $f_0 = (2\pi\tau_0)^{-1}$  is also shown. The calculated curve of  $\log S_M$  was vertically adjusted by a rigid shift.

of chain bonds. Even when the internal viscosity is suppressed, from comparison of the dash-and-dot curves in Figure 1 we see that some difference still exists. The reason is that the elastic tension along the chain is not transmitted by first-neighboring atoms only but to a minor degree by more separated atoms as well, as may be seen from analysis of the generalized characteristic ratio  $C(q)$ .<sup>12,14</sup>

Figure 1 also shows plots of  $\varphi_s$  and  $\varphi_\eta$  obtained from the simplified equations (28)–(30). Although they apply to the low-frequency limit  $\omega\tau_0 = 2\pi f\tau_0 \ll 1$ , here they are extrapolated to the whole frequency range. As may be seen for frequencies well below  $f_0 = (2\pi\tau_0)^{-1}$ , substantial deviations are observed from the plots derived from the full equations (21)–(22). In particular, at frequencies  $f \gtrsim 10^4$  s<sup>-1</sup>,  $\eta''$  and  $G''$  become negative (see also later), and so does  $\varphi_\eta$ . This unacceptable behavior of the elastic response indicates that the simplified expressions lose their physical meaning above this frequency.

Comparison of our calculations with experiment<sup>6,7</sup> is shown in Figures 2 and 3. In Figure 2 the OFB results of  $\varphi_s$  and  $\log S_M$  (see eq 35) are plotted versus  $f = \omega/2\pi$  from ref 6. Concerning  $\log S_M$ , we remark that this

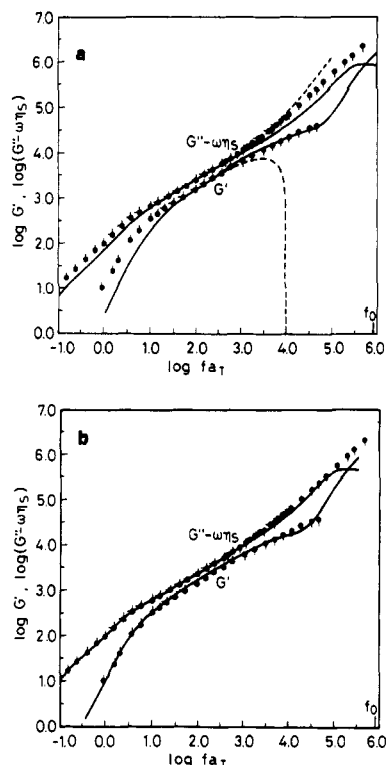


**Figure 3.** (a) Experimental and calculated complex modulus components  $G'$  and  $G'' - \omega\eta_s$  plotted as a function of the applied frequency (solid line, eq 22–27 and 35c). The curves calculated with the simplified expressions (eq 29, 30, and 35c) are shown with a dashed line. Experimental results are from atactic polystyrene,  $M_w = 8.6 \times 10^5$ , in Aroclor 1248,  $\rho = 0.0152 \text{ g cm}^{-3}$  (from ref 7). Numerical values of the parameters are given in the text and  $N$  is  $1.65 \times 10^4$ . A vertical, rigid shift was applied to the calculated curves. (b) Same as in (a) with the calculated curves rigidly shifted to the left by a factor 2.7 (see the text).

quantity is rather insensitive to internal viscosity unless we go to very high frequency. As for  $\varphi_s$ , agreement between theory and experiment is satisfactory up to  $f \approx 5 \times 10^4 \text{ s}^{-1}$ . We point out that the simplified expression apparently gives a better fit at high frequency in this plot but cannot describe correctly VE behavior, as said above (see also Figure 3a). At larger frequency, as  $f$  approaches  $f_0$  the theory becomes inexact in that it would require a more detailed treatment of the actual mechanism of relaxation. Quite apart from this remark, in this frequency region the experimental results show an anomalous behavior: in particular,  $\varphi_s$  becomes larger than  $90^\circ$ , implying that  $S' - S_s$  changes to negative. While to our knowledge no existing theory of polymer dynamics may account for such an effect, some degree of specific orientation of the solvent molecules in the immediate neighborhood of the chain has been suggested as its source.<sup>1,10</sup>

The experimental<sup>7</sup> and calculated results of the complex modulus (see eq 35) are reported in Figure 3a. Unlike the OFB plots of Figure 2, here the curves calculated according to the simplified equations (28)–(30) become strongly inexact even for frequencies 100 times small than  $f_0$ , with  $G'$  becoming negative, as mentioned before. Accordingly, in the following we shall refer exclusively to the results obtained with the complete expression given in eq 22. Apart from a rigid, vertical shift, no parameter was further adjusted, all of them being derived from the previous fit of the OFB results, except for the number of chain atoms that was chosen to correspond to the average molecular weight  $M_w$ . Although the agreement is less satisfactory than for the OFB data, we point out that a mere change of the friction coefficient per chain atom improves the fit,

bringing it to about the same degree as previously obtained by us using the same approach.<sup>3</sup> As shown in Figure 3b, this amounts to a logarithmic shift of the calculated plot toward lower frequencies, implying an increase by a factor 2.7 of the time unit  $t_0$  and therefore of  $\zeta$  (see eq 31). Although no simple physical reason may be proposed to justify this disagreement, we point out that a factor 2.7 is relatively modest in comparison with the change by more than 2 orders of magnitude undergone by the solvent viscosity  $\eta_s$ <sup>17</sup> during the experimental procedure, leading to the master curve through the time-temperature superposition criterion.

Overall, we see that the numerical values of the parameters used in our calculations are rather close to those previously obtained from fitting viscoelastic and scattering data from atactic polystyrene in various solvents.<sup>3,9</sup> It is interesting to note, however, that  $h_0$  is almost twice as large as what found in a previous paper<sup>3</sup> for the same polymer, namely, 0.055 versus 0.03, which implies that we are now a little closer to the Zimm limit of the impermeable coil. This finding is consistent with the remark that the solutions considered in the present study are more dilute than those in the quoted work,<sup>3</sup> being below, or perhaps close to, the overlap concentration. Therefore, some increase of  $h_0$  is to be expected in view of the reduction of intermolecular hydrodynamic screening at lower concentrations. Although this procedure is rather crude, we point out that a more comprehensive theory including both internal viscosity and finite concentration effects is still lacking.

The best-fit value of the rotational relaxation time,  $\tau_0 = 1.92 \times 10^{-7} \text{ s}$ , in Aroclor 1248 at  $T = 25^\circ \text{C}$  ( $\eta_s = 2.5 \text{ P}$ ), is especially interesting. Assuming strict proportionality between  $\tau_0$  and  $\eta_s$ , in agreement with the diffusive limit of Kramer's kinetic theory,<sup>15</sup> the reduced value of  $\tau_0$  for a benzene solution at  $25^\circ \text{C}$  ( $\eta_s = 6 \times 10^{-3} \text{ P}$ ) is  $0.46 \times 10^{-9} \text{ s}$ . This result derives from fitting of the OFB data, whereas from VE data we would have a 2.7-fold increase, namely,  $1.24 \times 10^{-9} \text{ s}$ , although the former result should be considered as more reliable. It is interesting that correlation times for local motions in polystyrene dissolved in benzene or toluene at  $25^\circ \text{C}$  have been determined to be in the range between  $0.2 \times 10^{-9}$  and  $4 \times 10^{-9} \text{ s}$  by several techniques (NMR,<sup>8</sup> ESR,<sup>18</sup> dielectric relaxation<sup>19</sup>), in agreement with our results. More specifically, a correlation time of about  $0.3 \times 10^{-9} \text{ s}$  derives from a dynamic description whereby each rotation involves three consecutive bonds; however, a more realistic model is likely to involve a longer correlation length, with the consequence that the correlation time may increase significantly.<sup>8</sup>

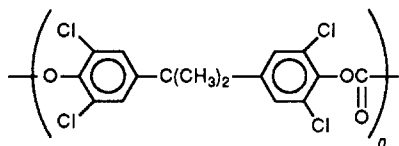
It should be reminded that the high-frequency behavior of polystyrene in Aroclor was already interpreted on the basis of the Cerf–Peterlin theory of internal viscosity.<sup>20</sup> While this approach may be very effective from a practical viewpoint, it relies on the definition of some parameters, most notably the so-called submolecule length, the numerical value of which may not bear a direct physical meaning. Conversely, we stress that the present approach is based on conformational and statistical grounds<sup>2,4</sup> and that the parameters are consistent with molecular structure and properties, with the partial exception of the numerical value of the hydrodynamic interaction parameter  $h_0$ , which is taken as close to currently adopted figures.

### Concluding Remarks

Oscillatory flow birefringence (OFB) and viscoelasticity (VE) results from atactic polystyrene (PS) in Aroclor 1248 solution are interpreted with a molecular theory based upon nonequilibrium statistical mechanics considerations.<sup>2,4</sup>

For frequencies  $f$  smaller than  $f_0 = (2\pi\tau_0)^{-1}$ , where  $\tau_0$  is the average relaxation time for skeletal rotations, a satisfactory agreement between calculation and experiment is obtained by using the actual (average) number of chain atoms  $N$  and a value of  $\tau_0$  that essentially agrees with the chain rotational correlation time obtained from NMR,<sup>8</sup> ESR,<sup>18</sup> and dielectric relaxation<sup>19</sup> data. For larger frequencies, a growing disagreement involving in particular the phase angle of the OFB response is observed (see Figure 2). We believe that solvent organization in the vicinity of the polymer chains, as first suggested by Lodge and co-workers,<sup>1,10</sup> may be the main reason of this discrepancy between calculation and experiment. In fact, for  $f < f_0$  each chain bond undergoes several rotations during each cycle of the applied strain, so that the solvent molecules are effectively distributed over a variety of arrangements, and the classical description of the solvent as a structureless continuum is applicable. Conversely, if the applied frequency is larger than the natural bond rotation frequency  $f_0$ , the chain tends to assume a locally rigid structure, which may favor specific arrangements of the surrounding solvent molecules. Interestingly enough, the solvent influence seems to be especially concentrated on the *phase*, rather than on the *modulus* of the dynamic response. This conclusion may be partly checked from Figure 2, where the calculated and the experimental values of  $\log S_M$  do not show significant deviations even at the largest frequencies, and it was especially apparent from a previous dynamical study of PS in solution, based on quasi-elastic neutron scattering data.<sup>9</sup> Here the half-peak time of the dynamic structure factor was well interpreted within the present theory and with about the same parameters as in the present study, down to observation times well below  $\tau_0$ . In this regard we remark that the half-peak time is an overall measure of chain relaxation at a particular scattering angle, irrespective of any partition between in-phase and out-of-phase components.

It may be worth pointing out that the typical maximum of  $\varphi_s$  at large frequencies, as resulting from our calculations, was indeed qualitatively observed at least in a couple of cases.<sup>10</sup> One example was found with freshly dissolved poly( $\alpha$ -methylstyrene): the maximum is reported to disappear gradually with time, giving rise to the steep increase of  $\varphi_s$  beyond 90°, similar to that reported in Figure 2 for polystyrene, after an interval of a few years. Incomplete solvation of the polymer chains in the freshly dissolved sample may be related with the observed effect, to the extent that it may imply limited solvent organization. Another example was found with the polycarbonate



although in this case the measurements were not repeated after a very long time.

As a last remark, we recall that in the same paper reporting the above results, Lodge and Schrag also compare results of  $\varphi_s$  for polystyrene and poly( $\alpha$ -methylstyrene) samples (see Figure 4 of ref 10) having the same number of skeletal atoms, under the same experimental conditions.<sup>10</sup> The latter polymer shows the characteristic uprise at lower frequencies, which is consistent with a value of  $\tau_0$  about twice that of polystyrene, in our theory. This result is in agreement with the expected larger energy barrier to skeletal rotation in poly( $\alpha$ -methylstyrene) than in polystyrene, due to the presence of the side methyl group in the former polymer.

**Acknowledgment.** One of us (M.A.F.) gratefully thanks the International Centre for Theoretical Physics (ICTP), Trieste, Italy, for a fellowship through the ICTP Programme for Training and Research in Italian Laboratories. This study was financially supported by Ministero della Pubblica Istruzione (40%), Italy.

**Registry No.** PS, 9003-53-6.

## References and Notes

- (1) See, e.g.: Martel, C. J. T.; Lodge, T. P.; Dibbs, M. G.; Stokich, T. M.; Sammler, R. L.; Carriere, C. J.; Schrag, J. L. *Faraday Symp. Chem. Soc.* **1983**, *18*, 173 and references therein.
- (2) Allegra, G. *J. Chem. Phys.* **1974**, *61*, 4910.
- (3) Allegra, G.; Ganazzoli, F. *Macromolecules* **1981**, *14*, 1110.
- (4) Allegra, G. *J. Chem. Phys.* **1986**, *84*, 5881.
- (5) Zimm, B. H. *J. Chem. Phys.* **1956**, *24*, 269.
- (6) Lodge, T. P.; Schrag, J. L. *Macromolecules* **1982**, *15*, 1376.
- (7) Massa, D. J.; Schrag, J. L.; Ferry, J. D. *Macromolecules* **1971**, *4*, 210.
- (8) Matsuo, K.; Kuhlmann, K. E.; Yang, H. W. H.; Gény, F.; Stockmayer, W. H. *J. Polym. Sci., Polym. Phys. Ed.* **1977**, *15*, 1347.
- (9) Allegra, G.; Higgins, J. S.; Ganazzoli, F.; Lucchelli, E.; Brückner, S. *Macromolecules* **1984**, *17*, 1253.
- (10) Lodge, T. P.; Schrag, J. L. *Macromolecules* **1984**, *17*, 352.
- (11) Brueggeman, B. G.; Minnick, M. G.; Schrag, J. L. *Macromolecules* **1978**, *11*, 119. Morris, R. L.; Amelar, S.; Lodge, T. P. *J. Chem. Phys.* **1988**, *89*, 6523.
- (12) Allegra, G. *J. Chem. Phys.* **1978**, *68*, 3600.
- (13) Allegra, G.; Ganazzoli, F. *Adv. Chem. Phys.* **1989**, *75*, 265.
- (14) Allegra, G.; Ganazzoli, F. *J. Chem. Phys.* **1981**, *74*, 1310.
- (15) Ganazzoli, F.; Fontelos, M. A. *Polymer* **1988**, *29*, 1648.
- (16) Kramers, H. A. *Physica* **1940**, *7*, 284.
- (17) De Mallie, R. B., Jr.; Birnboim, M. H.; Frederick, J. E.; Tschoegl, N. W.; Ferry, J. D. *J. Phys. Chem.* **1962**, *66*, 536.
- (18) Bullock, A. T.; Butterworth, J. H.; Cameron, G. C. *Eur. Polym. J.* **1971**, *7*, 445.
- (19) Mashimo, S.; Chiba, A. *Polym. J.* **1973**, *5*, 41.
- (20) Cerf, R. *J. Polym. Sci.* **1957**, *23*, 125. Peterlin, A. *J. Polym. Sci., A-2* **1967**, *5*, 179. Thurston, G. B.; Peterlin, A. *J. Chem. Phys.* **1967**, *46*, 4881.